Renewable Energy 85 (2016) 766–776

Contents lists available at ScienceDirect

Renewable Energy

journal homepage: www.elsevier.com/locate/renene

Climatic cooling potential and building cooling demand savings: High resolution spatiotemporal analysis of direct ventilation and evaporative cooling for the Iberian Peninsula

Hugo Campaniço [a,*], Pedro M.M. Soares [b], Pierre Hollmuller [c], Rita M. Cardoso [b]

[a] University of Lisbon, DEGGE, Campo Grande, Ed. C8, 1149-016 Lisbon, Portugal
[b] Instituto Dom Luiz, University of Lisbon, Lisbon, Portugal
[c] Institut Forel, Section of Earth and Environmental Sciences, University of Geneva, Switzerland

ARTICLE INFO

Article history:
Received 19 November 2014
Received in revised form
13 June 2015
Accepted 14 July 2015
Available online xxx

Keywords:
Passive cooling
Climatic cooling potential
Cooling demand savings
Renewable energy resources
Iberian Peninsula

ABSTRACT

In the present study a new methodology allowing the assessment of building's cooling demand savings by the use of ventilated passive cooling systems is presented in a twofold innovative way. Firstly, using a redefined concept of the climatic cooling potential (CCP), which allows for the direct estimation of savings in building's cooling demand by the use of different passive cooling systems on a large spatio-temporal scale. Secondly, this assessment relies on high resolution climate dataset built using a regional climate model covering the Iberian Peninsula (IP) with a 9 km horizontal spacing and the period between 1989 and 2008. Here, the CCP concept is applied for direct ventilation and evaporative cooling, in such a way that it allows for a comparison with the building monthly cooling demand, providing a direct assessment on the cooling demand savings for any building, for three air flow rates. The results show that CCP is asymmetrically distributed both spatially and temporally within the IP. During the cooling season CCP values are above 1 kWh per m^3 of building and 3 kWh per m^3 of building, for direct ventilation and evaporative cooling, respectively. Evaporative cooling provides a less heterogeneous annual cycle of CCP than direct ventilation, with a relative difference in the south and central part of the Iberian Peninsula superior to 100% during summer. Nonetheless, despite the consistently higher values offered by evaporative cooling, in the coastal regions the relative difference between the two systems drops to less than 10% due to the higher moisture in the air. For the case of a typical office room in the region of Lisbon, in the month of August, the cooling demand savings provided by the use of direct ventilation and evaporative cooling can represent more than 27% and 40% of the cooling demand, respectively.

1. Introduction

1.1. Direct ventilation and evaporative cooling

In 2012 buildings were responsible for nearly 40% of the final energy consumption in Europe, placing the building sector as the biggest energetic consumer, above industry (31%) and transportation (26%) [1]. The rapid increase in electricity demand for air-conditioning associated with the global warming issue, will further boost the primary energy demand for building cooling [2–5]. In the current energy paradigm, this will enhance even more the anthropogenic CO_2 emissions and therefore global warming with its environmentally and societal harmful consequences. The use of renewable energy resources such as the passive cooling systems and their implementation in buildings is mandatory to overcome the current energy paradigm, since they can be an important solution to contribute to minimize buildings cooling loads and thus the fossil fuel dependence. The effectiveness of passive cooling systems has been widely documented through several studies [6–8], however, here we focus only on direct ventilation and evaporative cooling.

Direct ventilation techniques are one of the most used, widely known and simple passive cooling techniques. Whenever there is cooling demand inside a building and the outside temperatures are lower than the building's set point temperature, then the outside air can be brought inside, reducing its temperature and cooling load. The air can flow inside by the use of fans (mechanically

* Corresponding author.
E-mail address: hugo.campanico@alunos.fc.ul.pt (H. Campaniço).

http://dx.doi.org/10.1016/j.renene.2015.07.038
0960-1481/© 2015 Published by Elsevier Ltd.

Nomenclature

CCP	climatic cooling potential (kWh/m^3 of ventilated building)
c	heat capacity of air (kWh/K kg)
ρ	air density (kg/m^3)
v	ventilation flow rate (air changes per hour)
v_{ref}	standard ventilation flow rate (kg/h or air changes per hour)
v_{vnt}	passive cooling system's ventilation flow rate (kg/h or air changes per hour)
T_{bld}	building temperature (°C)
T_{vnt}	passive cooling system output temperature (°C)
T_{set}	building's set point temperature (°C)
T_{ext}	outdoor temperature (°C)
UCP	useful cooling potential (kWh/m^3 of ventilated building)
Qcool	building's cooling load (kWh)
ΔQcool	effective savings (kWh)
η	evaporative cooling system's efficiency
T_{wb}	wet bulb temperature (°C)
ach	air changes per hour (h^{-1})

forced), using the naturally available thermal gradients through openings (natural) or both ways [9]. Direct ventilation is often used during the night and hence commonly referred as night cooling. As recognized in many studies, direct ventilation can be extremely efficient in the reduction of the cooling loads [10–14], though the efficiency is mainly related to the difference between indoor and outdoor temperatures, the air flow rate, the building's thermal mass [11] and cooling demand.

Evaporative cooling is a process where an air flow is forced through a humid membrane or a water surface absorbing some of the water; thus its temperature is reduced through the release of latent heat of vaporization for the change of state of the water molecules from liquid to gaseous. Evaporative cooling can be direct or indirect. In direct evaporative cooling the humidified air is transported directly into the building. Due to the possibility of condensation inside the building, the air can be forced through a membrane allowing for the separation of the water vapour from it. In the case of indirect evaporative cooling, the cooled humidified air is forced into a heat exchanger maintaining its levels of humidity and at the same time decreasing its temperature and lowering the risk of condensation [15]. Evaporative cooling techniques have been proved feasible both from economic and technical stand points through numerous studies [16–19], nevertheless their efficiency can dramatically be reduced in the case of hot humid climates. Nonetheless, it is expected that indirect evaporative cooling systems will represent near 20% of air-conditioned market in buildings over the next 20 years world-wide [20].

1.2. Climatic cooling potential

A major obstacle for the implementation of passive cooling systems is related to the necessity of using building thermal simulation or in situ measurements to assess their viability for a particular case, which in both cases are time consuming processes, require expertise and detailed knowledge of building simulation tools which are expensive, making it inaccessible for most of the building designers. In order to address this problem Artman et al. [9] suggested a new integrated index, named Climatic Cooling Potential (CCP), defined as the summation of the products between building and external air temperature difference and the time interval. The CCP gives a measure of the climatic availability for cooling. In the later study, CCP was computed for the night period across Europe using observations for the main cities, allowing an evaluation of the climatic availability for the use of night cooling in those European cities. Nonetheless, this method does not provide information on how effective this potential could be, or which part of the CCP can really be used to lower the building cooling loads. The main shortcomings of the latter study are: firstly, high CCP values may have in fact very low or none utility in case of absente cooling loads; secondly, CCP was only computed for the night period, neglecting some eventual CCP availability during the day. In fact, there are very few studies focused on the potential for passive cooling techniques which are not based on building thermal simulation. Studies based on building thermal simulation provide quantitative information on cooling demand savings by the use of passive cooling systems, but only for specific cases. Other studies, not relying on building thermal simulation, do not provide quantitative information on the effectiveness of the climatic cooling potential and do not relate it to the cooling demand savings [21–23].

Recently, Campaniço et al. [24] were the first to compute a climatic cooling potential for passive cooling systems in a way that it can be directly related to cooling demand savings independent of any building characteristic and without the use of building thermal simulation. In this study, CCP was computed for complete diurnal cycles and then compared to data for building cooling demand, to achieve the cooling demand savings through a simple model. The model was tested against an extensive set of numerical simulation experiments, combining several passive cooling possibilities with different building configurations and meteorological data, resulting in a total of 7776 different cases. The referred model, named Useful Passive Cooling model (UPC) uses as input the building cooling demand for a certain time period (hourly, daily, weekly and monthly values) and then compares it to the CCP for the same time period. It was found that the minimum value between CCP and building cooling demand (UCP) was very close to cooling demand savings. In fact, for a daily accumulation period, due to the typical building's characteristic time constant, UCP is fairly equal to cooling demand savings, with less than 1% error on average. However, good results are also achieved for monthly cooling demand values, with 11% average overestimation of savings for all cases. The results showed unequivocally that the model is a remarkable tool to assess the cooling demand savings in buildings by the use of ventilated passive cooling systems without the use of building's thermal simulation and independently of building properties. Here we redefine and apply the concept of the CCP in an innovative way, which allows for the direct estimation of savings in building's cooling demand by the use of any ventilated passive cooling system for any building and spatiotemporal scale. The methodology and the concepts presented here are applied for the Iberian Peninsula (IP) for evaporative cooling and direct ventilation, nonetheless, they're valid and applicable for any region and ventilated passive cooling system.

1.3. Climate models

Global numerical weather prediction models led to the development of an increased number of global climatological datasets like the reanalyses from the European Centre for Medium Range Forecasts (ECMWF) ERA-40 [25] and ERA-Interim [26], from the National Centres for Environmental Prediction [27], and the Twentieth Century Reanalysis Project [28], and others. Simultaneously, a large number of Global Climate Models (GCMs) have been used to build climate change scenarios. This effort has been fruitful in generating global climatic information for the 20th century in easy to use regular or quasi-regular grids.

Reanalysis and climate scenario datasets have coarse horizontal resolutions, typically between 1° and 4° (in both latitude and longitude), good enough to reproduce many aspects of large-scale climate [29], but unable to represent many processes and systems that drive regional and local climate variability, where the consequences of climate change will be mostly felt. These limitations are greatly amplified in areas of difficult geomorphology, like complex orography, irregular coastlines, and regions with heterogeneous land cover, where regional and local thermal and mechanical circulations are forced by surface heterogeneity.

To overcome these problems, different downscaling approaches have been advanced. Statistical methodologies [30] use observed relationships between variables at different scales to estimate finer scale properties, but have a major drawback: the observed relationships may not persist in a changing climate. Regional climate models (RCMs) constitute an increasingly popular alternative [31–35]. RCMs, forced by GCMs or by reanalysis data, are able to capture physically consistent regional and local circulations [36–40] at the required horizontal and temporal scales, allowing for the development of high-resolution climatologies in any terrain conditions, and when forced by reanalysis fill the gaps of observational networks. Results from different RCMs forced by ERA-40 reanalysis, like those of PRUDENCE [34,41] and ENSEMBLES [42] European projects are a valuable source of atmospheric data for Europe, and in particular for Iberia. Furthermore, results from high resolution RCMs forced by ERA-interim constitute the best climate datasets for Europe and in particular for the Iberia, and have been used very successfully for different economic sectors, like agriculture, forestry and especially renewable energy sources. These climate datasets are used to characterize the present resource in a very detailed manner and to assess the climate change impact on the referred sectors. The added value of these results is both due to the detailed spatial resolution and the time sampling used, allowing the production of hourly data crucial for wind energy, solar energy and potential climatic cooling assessment.

1.4. Objectives and outline

The methodology presented in this study has been designed to explore the value of quality climate data, either observational or from regional climate modelling, enabling for the direct assessment of building's cooling demand savings by the use of ventilated passive cooling systems. From this new innovative methodology it is possible to obtain a preliminary estimation of the cooling demand savings provided by each of the passive systems considered, for different air flow rates (associated to the passive systems) for any climate or region without the need to use building thermal simulation and in a way independent of any building properties. We apply this methodology for direct ventilation and evaporative cooling to a high quality present climate dataset covering the Iberian Peninsula (IP), generated using a state-of-the-art regional climate model, having a high spatial resolution. In the following section we will present the referred methodology and in Section 3 the description of the meteorological input that is used to create the database that allows for the estimation of cooling demand savings in the IP, which is shown in Section 4 along with a comparison between the two systems and a sensitivity analysis to the passive cooling system's air flow rate. Finally, at Section 5, we present the main conclusions of the present study.

2. Methodology

The method used in the present study closely follows Campaniço et al. [24], however, here we characterize any given passive cooling system based on ventilation in terms of its climatic cooling potential CCP in such a way that allows for the assessment of the cooling demand savings provided by it use for any building for any spatiotemporal scale, which was not established in Campaniço et al. [24]. In the referred study, CCP was determined in order to allow to compute the cooling demand savings by the use of different passive cooling systems based on ventilation for a specific case/building, here, this climatic index is redefined in such a way that it permits to access the cooling demand savings by the use of different passive cooling systems based on ventilation but for a large spatiotemporal scale and for any building. The CCP relates the temperature of the cooling source T_{vnt} and the associated air flow rate v, to the cooling load which a passive cooling system brings to a building at temperature T_{bld}, in reference to ventilation at standard reference air flow rate v_{ref} from outside:

$$CCP = c\cdot\rho\cdot v\cdot(T_{bld}-T_{vnt}) - c\cdot\rho\cdot v_{ref}(T_{bld}-T_{ext})$$
$$v = \begin{cases} v_{vnt} & if \quad T_{vnt} < T_{bld} \\ v_{ref} & if \quad T_{vnt} \geq T_{bld} \end{cases} \tag{1}$$

Note that: (i) the system may be designed at a higher flow rate v_{vnt} than the standard flow rate v_{ref}, enhancing the cooling load, but should be reduced to v_{ref} when the source temperature is higher than the building; (ii) the flow rates which are used here are building specific (in terms of air change per hour), so that the *CCP* is expressed in kW per m^3 building (or kWh per m^3 building when integrated over a certain period).

In absence of prior knowledge of the building response, the above defined CCP is actually evaluated at a comfort set point T_{set} (instead of T_{bld}). It is in this sense that the CCP represents a climatic index (dependent on the climate under consideration, the passive cooling system and the flow rate, as well as the comfort set point), independently of any building characteristics.

Since the CCP is a climatic index, it will at certain times be higher than the actual cooling load of the building (in particular during the winter season, but possibly also at certain periods of the summer, typically at night). For assessment of the effective contribution, in terms of thermal energy savings for a particular building, the CCP must hence be compared to the cooling load Q_{cool} in absence of passive cooling which is needed for the building temperature not to rise above T_{set}. This comparison, which is done over a certain integration time step, allows the reduction of the CCP to the useful cooling potential *UCP* for the particular building. Depending on the integration time step, we hence define the annual useful cooling potential as follows:

$$\begin{aligned}
UCP_{hourly} &= \sum_{h=1}^{8760} MIN(CCP, Q_{cool}) \\
UCP_{daily} &= \sum_{d=1}^{365} MIN\left(\sum_{h=1}^{24} CCP, \sum_{h=1}^{24} Q_{cool}\right) \\
UCP_{weekly} &= \sum_{w=1}^{52} MIN\left(\sum_{h=1}^{7\times24} CCP, \sum_{h=1}^{7\times24} Q_{cool}\right) \\
UCP_{monthly} &= \sum_{m=1}^{12} MIN\left(\sum_{h=1}^{30\times24} CCP, \sum_{h=1}^{30\times24} Q_{cool}\right)
\end{aligned} \tag{2}$$

In this respect, one of the crucial points is to determine the temporal precision at which the cooling system (CCP) and separately the building (Qcool) have to be characterized. In principle, the suitable choice of the integration time step for comparing CCP and Qcool relates to the thermal inertia of the building. As a matter of fact, when there is no cooling demand from the building and a certain cooling potential is present (in particular for direct night cooling), the latter can be stored into the building thermal mass for subsequent use, which is not taken into account by a too small integration time step (in particular hourly). On the other hand, a too long time step will lead to overestimation of the passive cooling load that can effectively be absorbed by the building.

For this sake, the simplified method presented by Campaniço et al. [24] was tested against an extensive numerical simulation campaign [24], concerning: (i) the case of an administrative building located in Geneva, with a variety of constructive and operational configurations (solar protection, thermal mass and insulation, internal gains); (ii) an important set of passive cooling techniques (direct ventilation, evaporative cooling, air-soil heat exchangers, thermal phase-shifting, as well as combination thereof) with diverse sizing and flow rates.

For the 7776 configurations, correlation between the two methods was analysed in terms of annual cooling energy savings. It was shown that calculation of the UCP on an hourly basis underestimates the effective savings by an average of 31%, due to the fact that the building thermal inertia is not taken into account, while calculation of the useful cooling potential on a daily basis reproduces the effective savings with less than 1% error in average. Calculation on a weekly or monthly basis tends in turn to overestimate the effective savings (average of 6% and 11%), due to overestimation of the available thermal inertia. The dispersion in relation to these averaged values was analysed for the particular case of daily and monthly calculation basis. Focus was set on the passive cooling fraction (fraction of the cooling demand which can be covered by the passive cooling system). It is shown that, if the data is available in monthly values, the model will tend to overestimate the passive cooling fraction. The error however remains below 20% for half of the cases, although it may be quite more important (up to 70% for extreme cases, in particular in cases where the model indicates close to 100% coverage and the associated cooling demand is low). As a main result, the new method of Equation (1), can therefore be used for setting up of a climatic potential database in a monthly time step, for roughly assessing the potential of these passive cooling techniques on a large spatio-temporal scale (some hundreds or thousands of km, some decades), for which integrated building simulation becomes prohibitive. Much more precise results could be obtained with data on daily resolution (less than 6% error in half of the cases), which however would require the setting up of a very extensive database of the climatic potential and the knowledge of hourly cooling demand. In this respect, finer evaluation of a particular case should rather use integrated simulation of the passive cooling system and building in hourly time step.

On the basis of preceding results we will now establish a CCP database for the Iberian Peninsula (IP), on monthly basis, concerning direct ventilation and evaporative cooling.

As climatic input, a 19 years high resolution hourly climate dataset for the IP mainland is used (see Section 3). In the case of direct ventilation, T_{vnt} is given by the dry bulb ambient air temperature, T_{ext}, while evaporative cooling is simulated with a constant efficiency η of 50% (in relation to the wet bulb temperature T_{wb}):

$$T_{vnt} = T_{ext} + \eta(T_{wb} - T_{ext}) \tag{3}$$

On the basis of Equation (1) the CCP will be computed for the case of a comfort set point T_{set} of 26 °C, with a reference flow rate v_{ref} of 1.5ach (of 1.5 m^3/h per m^3 building) during daytime (7 h–19 h), dropping to zero during the night (representative of an administrative building). The passive cooling system will be assessed for 3 different design flow rates v_{vnt}: (i) 1.5ach (same as the reference case, but also activated at night if T_{vnt} is below T_{set}); (ii) 3.0ach (reduced to reference if T_{vnt} is higher than T_{set}); (iii) 6.0ach (with same controlled reduction).

Given CCP one can easily assess the monthly energy savings provided by the passive systems simply by computing the product between $UCP_{montlhy}$ (Equation (2)) and the building's volume (m^3 of ventilated building).

3. Climate data

The current paper uses surface meteorological data from a high resolution climate simulation, performed with the state-of-the-art atmospheric model. The Weather Research and Forecasting (WRF) model (Skamarock et al., 2008) [43] used is a non-hydrostatic model, suitable for simulating a wide range of scales, from large eddy simulation to mesoscale model, with a large number of available options for the model core and the physical parameterizations, making it very competitive for numerical weather prediction, mesoscale meteorological studies and building the high quality climate dataset. The WRF version used here corresponds to its 3.1.1 cycle. Recently, WRF has been extensively used for dynamical downscaling for regional climate studies [44–51] revealing very good performance in generating hind casts to applications on the energy sector, for wind power, hydropower and moisture recycling (Rios-Entenza et al., 2014) [52].

For this study, WRF was setup with two grids, a parent one at 27 km (WRF27 km) and a second nested at 9 km (WRF9km) horizontal grid spacing, using one-way nesting. Both grids are centred in the Iberian Peninsula and have, respectively, 162 × 135 and 144 × 111 grid points, covering the regions shown in Fig. 1. In both domains 49 vertical levels are used, placing roughly 20 vertical levels in the planetary boundary layer, with the lowest model sigma level at approximately 10 m of height and model top at 50 hPa. The outermost domain was designed to cover a relatively large ocean area, reducing spurious boundary effects in the inner region. The WRF model run was set to start at 0000UTC (Universal Time Coordinated) 1 January 1989 and end at 2300UTC 31 December 2007. Initial and lateral conditions for the outer domain were derived from the ERA-Interim pressure-level reanalysis (Berrisford et al., 2009) [26]. The lateral boundary conditions and sea surface temperatures were both updated every 6 h, from ERA-Interim. In both domains 11 grid points are used as lateral relaxation areas. A complete and more detailed description of the model set-up can be found in Soares et al. (2012) [53] and Cardoso et al. (2013) [54], where the simulation results were extensively validated for inland maximum and minimum temperatures and precipitation, showing a remarkable agreement with either local or gridded observations. This simulation is one of the most valuable climate dataset at high resolution for Iberia, containing hourly data for numerous meteorological variables. For the present study, the variables used are: surface temperature (2 m), specific humidity (2 m) and surface atmospheric pressure. For all these variables the hourly sampling was used to compute the CCP, direct and evaporative.

4. Results and discussion

4.1. Direct ventilation vs evaporative cooling

In this section, the methodology presented previously (Section 2) is applied for direct ventilation and evaporative cooling, and CCP is mapped for the IP over 21,870 locations. The rate of ventilation for the passive systems and reference cases (v and v_{ref} of Equation (1)) are set at 1.5ach. However, a sensitivity analysis to the air flow rate is conducted at Section 4.2. Figs. 1 and 2 show the monthly average values of the CCP for direct ventilation and evaporative cooling, as well as standard deviation over the 1989–2008 period.

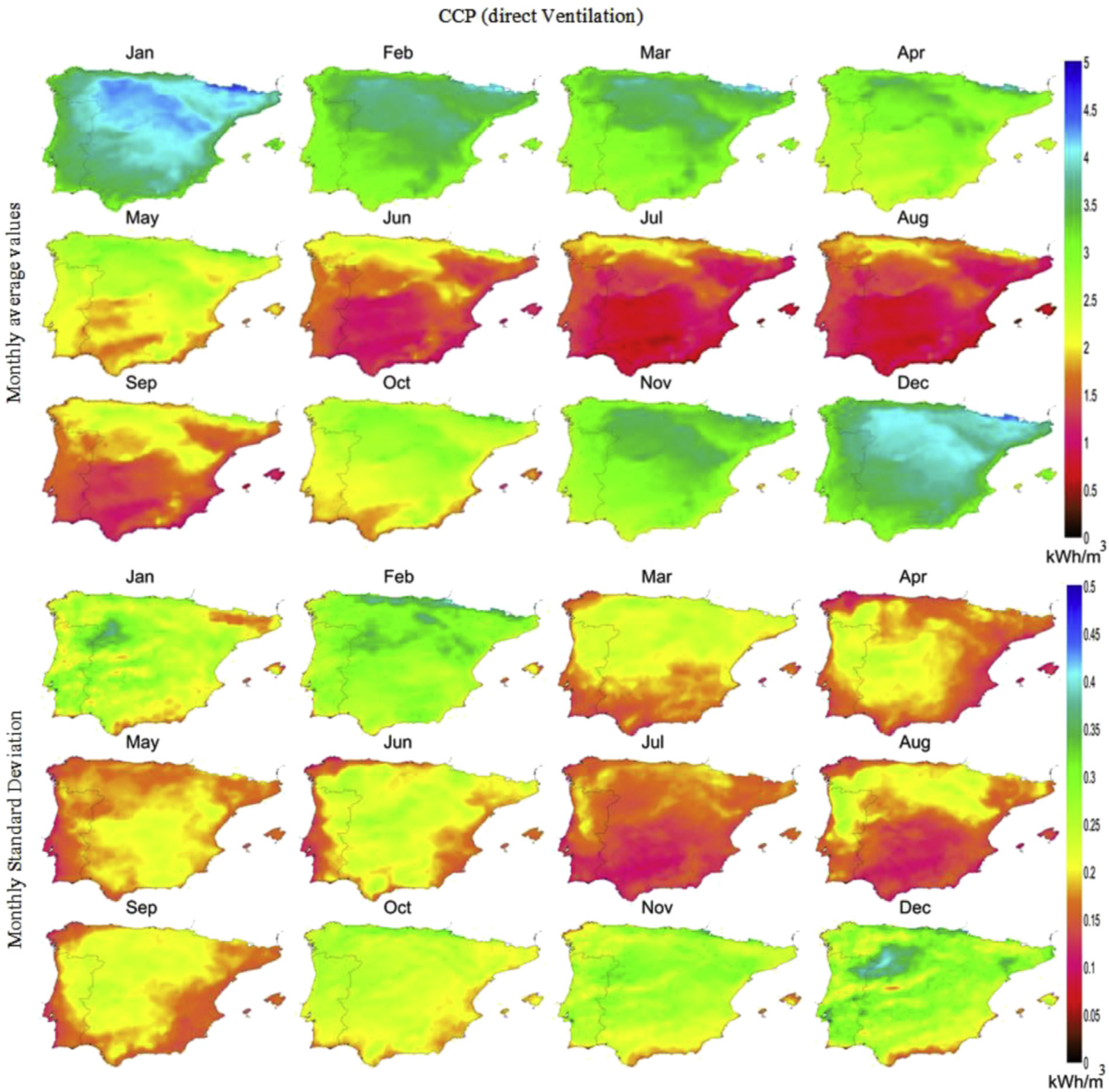

Fig. 1. Direct Ventilation's CCP for reference and passive rates of ventilation of 1.5ach. Top: CCP's monthly average values; Bottom: CCP's monthly standard deviation, for the period 1989–2008.

The CCP is given in kWh/m^3 (kWh per m^3 of ventilated building).

Regarding direct ventilation, Fig. 1 shows that CCP is generally above 2.5 kWh/m^3 in winter (October to March) over the entire IP, reaching 4 kWh/m^3 in the Pyrenees and the Iberian Cordillera from November to March. However, during summer, were the CCP is of higher utility, these values tend to diminish. At the beginning of the summer the average CCP is of 2.0 kWh/m^3 falling to 1.3 kWh/m^3 when considering all summer (April to September). The spatial heterogeneity of CCP is also evident in Fig. 1, showing higher CCP values in the north part of the IP (generally above 1.5 kWh/m^3 during all summer) and lower values in the south part, mostly bellow 1 kWh/m^3, with the exception of April and May due to lower temperatures. The IP's orography seems to have a significant effect in CCP, particularly in summer: the low altitude regions, as the Guadalquivir and the Ebro basins present lower CCP values, normally bellow 1 kWh/m^3, contrary to the high altitude regions, like the Pyrenees and the Iberian Cordillera where CCP is higher, usually above 2 kWh/m^3. Moreover, CCP tends to be lower at the southeast coastal regions of the IP due to higher temperatures of the Atlantic and the Mediterranean Sea during this same period. The standard deviation values of Fig. 1 (bottom) show a distinct spatial heterogeneity over the entire year and a trend for lower values during summer, where the standard deviation maximums are near 0.3 kWh/m^3 with an average of 0.14 kWh/m^3. For this period, the standard deviation represents a maximum of 11% relatively to the average CCP.

Concerning evaporative cooling, a similar picture can be found (Fig. 2). Like direct ventilation, during winter, were the temperatures are lower, CCP is higher, generally above 3 kWh/m^3 over all the IP. However, in this case, the CCP's spatial homogeneity is clearly higher during all year. Moreover, with the exception of the southeast coast, the average inter-annual amplitude of the evaporative cooling's CCP is near 2.5 kWh/m^3, instead of 4.5 kWh/m^3 (case of direct ventilation). Furthermore, for the majority of

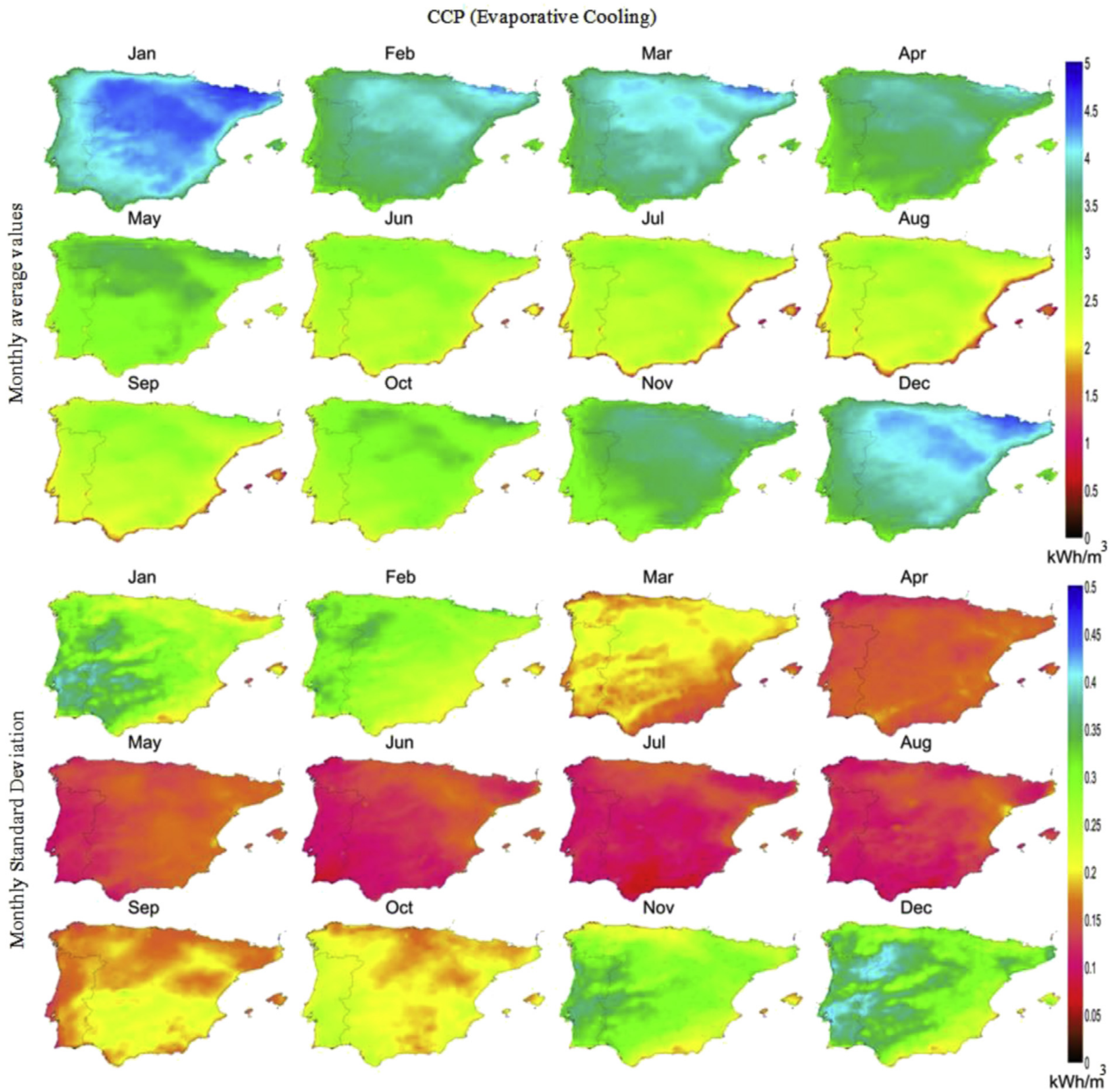

Fig. 2. Evaporative Cooling's CCP for reference and passive rates of ventilation of 1.5ach. Top: CCP's monthly average values; Bottom: CCP's monthly standard deviation, for the period 1989–2008.

summer (June to September) the CCP's spatial distribution along the IP as well as its average is quite similar from month to month, with most of its values above 2.0 kWh/m^3. Contrary to direct ventilation, were the IP's orography influence in CCP is more pronounced, in the case of evaporative cooling, the regions of the Guadalquivir and the Ebro's basins do not show substantially lower CCP during summer. Similarly, the regions of higher altitudes such as the Pyrenees and the Iberian Cordillera do not present noticeably higher CCP values relatively to other regions. Nonetheless, for the evaporative cooling there is a more distinct coastal effect, i.e. the proximity to the Ocean causes evaporative cooling's CCP to be substantially lower on southeast coast due to higher moist in air. This effect, combined with the warmer currents of the Atlantic and Mediterranean sea, causes the lower CCP values displayed during summer in the southeast coast of Fig. 2 (~1.5 kWh/m^3). Nevertheless, for the same periods and locations, evaporative cooling provides consistently higher CCP values than direct ventilation (see Fig. 3). One of the reasons is due to the duration during which CCP is available: Figs. 1 and 2 were produced with equal design and reference flow rates (v_{vnt} and v_{ref}), hence the CCP for direct ventilation is only available at night, when ventilation from outdoor can continue as compared to the reference case. For evaporative cooling, the ventilation temperature is lower than ambient, therefore the cooling potential (as compared with the reference) doesn't drop to zero during day time.

In order to better access the difference between evaporative cooling and direct ventilation, Fig. 3, expresses the relative difference between the CCP from evaporative cooling and direct ventilation.

During the winter the relative difference between the systems is between 2% and 69% with an average of 14%. However, during the summer, the discrepancy between the systems increases importantly. For the warmest months, in the climatological summer (June to August), the relative difference between evaporative cooling and

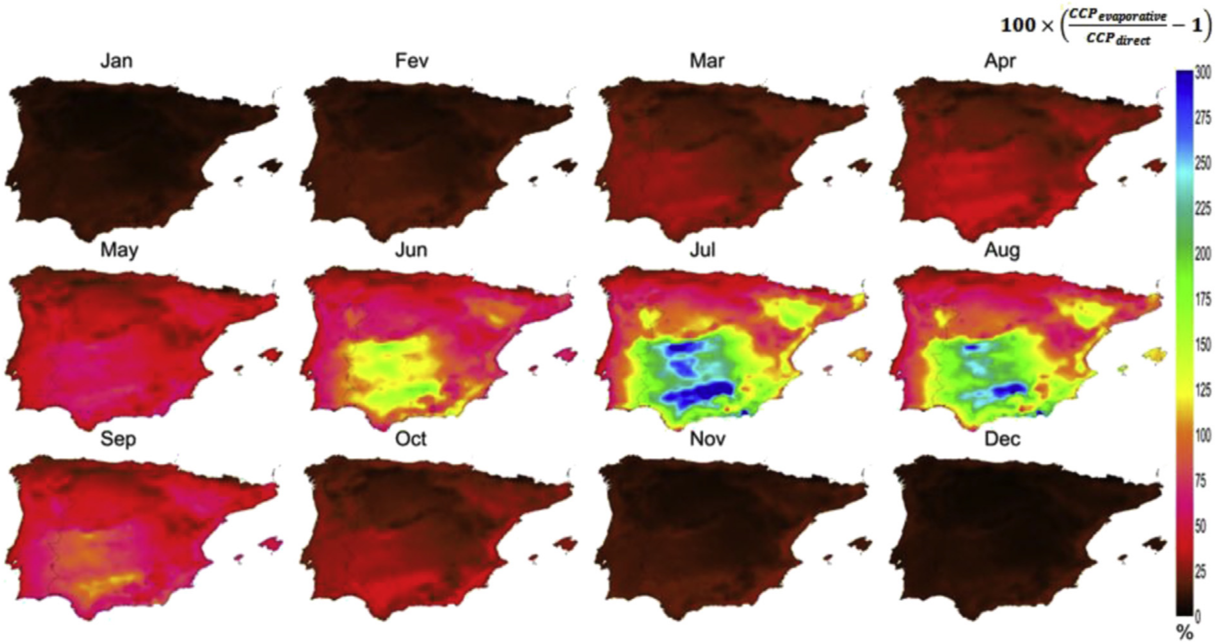

Fig. 3. Relative difference (%) between CCP for evaporative cooling and direct ventilation for 1.5ach reference and passive rates of ventilation.

direct ventilation is usually above 50%, furthermore, at the south central part of the IP the evaporative cooling system may provide 100% more CCP than direct ventilation, reaching local values above 250%. Nevertheless, for some regions, predominantly in the coast, due to high levels of air ocean moisture, the difference can be inferior to 11% in the full annual cycle.

Fig. 4 shows the mean monthly values of the relative difference of Fig. 3, for two specific illustrative locations, one in the coast (Mañón, Bares, Spain: 43°44′22″ N; 7°42′35″ W) and the other in the interior of the IP (Castelo Branco, Portugal: 39°48′39″ N; 7°30′28″ W). It can be seen that there is very significant difference in using evaporative cooling in relation to direct ventilation between a coastal location and an inland one. The annual cycle of improvement using evaporative cooling in a coastal location presents a small average value mostly constant, around 10%, i.e. with reduced amplitude, in the range between 9 and 13%, in May and September, respectively. The inland location, however, shows an average value of relative difference 50% higher for the full year. More importantly, during the summer the discrepancy between the two locations is remarkable, the average value is 95% larger, but the annual amplitude is also more noticeable due to the proximity between the inland and coastal ratios during winter, were evaporative cooling tends to be less effective relatively to direct ventilation.

4.2. Sensitivity to air flow rate

In the previous section the rate of ventilation was set at 1.5ach for the reference rate and for the passive cooling systems, however higher rates of ventilation can be used. To understand the effect of increasing the rate of ventilation, we conduct a sensitivity analysis for 3.0ach and 6ach air flow rates for both passive cooling systems.

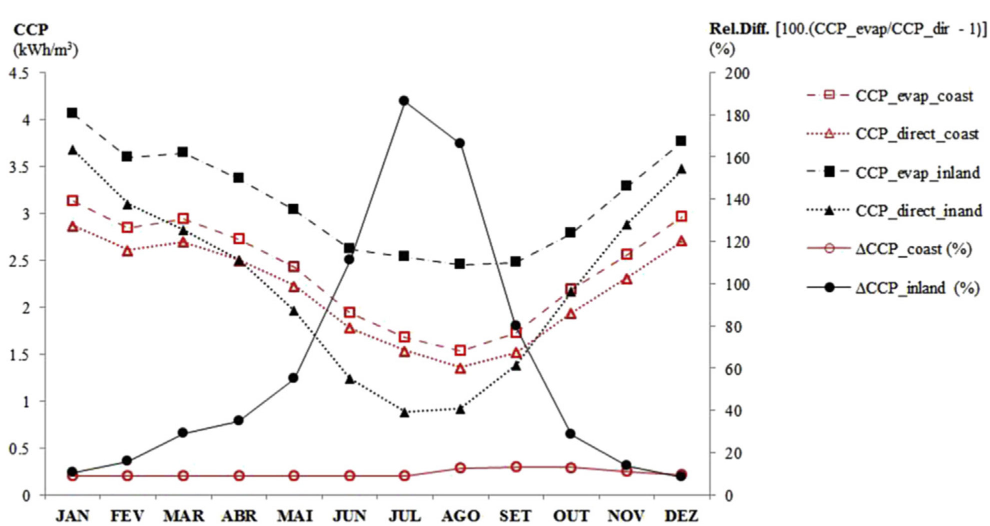

Fig. 4. Relative difference (%) between CCP for evaporative cooling and direct ventilation for 1.5ach reference and passive rates of ventilation for a region in the coastline and in the inland of the IP.

The reference rate of ventilation (v_{ref}) is kept at 1.5ach. The CCP spatial structure (not shown here) is similar to the ones presented on Figs. 1 and 2. To illustrate the scale factors between the different flow rates, the ratio between the CCP for 3.0ach and 1.5ach, as well as for 6.0ach and 1.5ach was computed for each IP grid point (near 22,000 locations) for direct ventilation and evaporative cooling. As a summary, the different statistical measures of these ratios, namely the absolute extremes, quartiles, median, average and standard deviation are calculated for monthly values for both systems, for the full meteorological model database (Figs. 5 and 6).

In the case of direct ventilation, Fig. 5 shows clearly the non-linear gain of using higher ventilation rates (see Equation (1)). Doubling and quadruplicating the ventilation rates leads to an annual average ratio's increase of 3.1 and 7.2, respectively. In fact, for the 3.0/1.5ach ratio of direct ventilation, the monthly average values in the annual cycle are roughly constant, with an annual average equal to 3.1, reaching a maximum of 3.5 in August and a minimum of 2.2 in July. The monthly range of the sample varies from 0.37 in December to 1.29 in August. Standard deviation achieves its minimum of 0.08 in December and its maximum of 0.34 in July, which represents only 11% of the average value for the same month. For the 6.0/1.5ach ratio the annual average is 7.2 and the monthly ranges of the sample are wider, varying form 1.1 in December to 3.8 in August. The standard deviation values are also higher, ranging from 0.23 in December to 1.01 in July, however, the maximum relative difference from the monthly average is only of 15% (for July). Also, a greater interquartile distance is visible in the summer, which causes standard deviation vales to be higher.

For the 3.0ach/1.5ach ratio of the evaporative cooling case (Fig. 6) the monthly ranges are similar to direct ventilation but with greater standard deviation values, between 0.06 (December) and 0.48 (July), however, in the case of the 6.0/1.5ach ratio the monthly ranges are higher, varying from 1.2 in December to 4.7 in July, as well as the standard deviation, which varies from 0.19 in December to 1.4 in July.

In Fig. 7 the relative difference from evaporative cooling and direct ventilation is displayed for the same inland and coastal locations of Fig. 4, for 3.0ach and 6.0ach passive flow rates along the full annual cycle. The relative difference between evaporative cooling and direct ventilation diminishes with the increased air flow rate of the passive systems. This decrease is more pronounced when comparing the 3.0ach and 1.5ach air flows than the reduction from 6.0ach to 3ach, since at 1.5ach there are some periods when the direct ventilation corresponds to the reference flow rate.

4.3. Assessing useful cooling potential

In order to assess the UCP for a specific building one needs to know its cooling demand and volume. As an example, here we proceed to thermal simulation of two office rooms (undermentioned as “A” and “B”) located in the region of Lisbon using TRNSYS [55]. The office rooms are 20 m^2, 50 m^3, south orientated, with 20 W/m^2 internal gains. The air renovation flow rate is of 1.5ach during occupation (7 h–19 h). Building “A” has 50% glazing area without any kind of solar protection (overall g value of 68%), while building “B” has 50% glazing with exterior solar protection

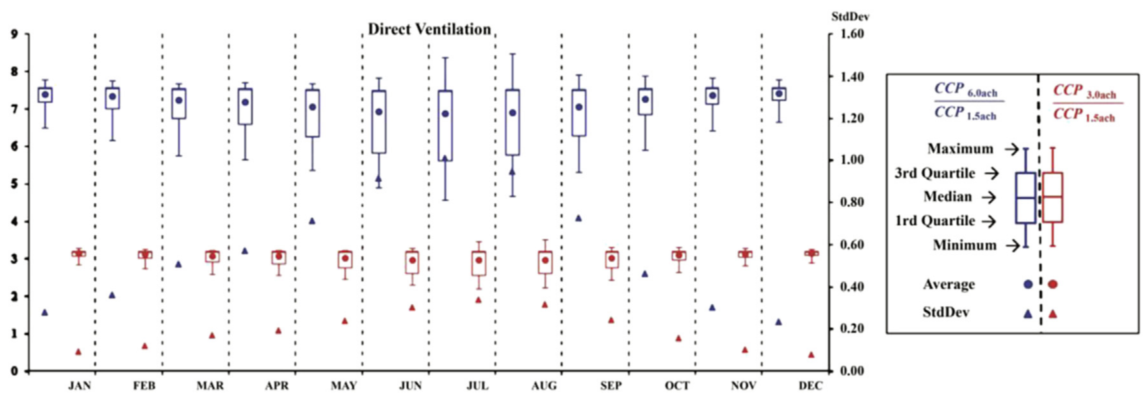

Fig. 5. Spatial statistics of CCP for direct ventilation: ratio between CCP for 6.0 and 1.5ach (black) and between CCP for 3.0 and 1.5ach (red).(For interpretation of the references to colour in this figure legend, the reader is referred to the web version of this article.)

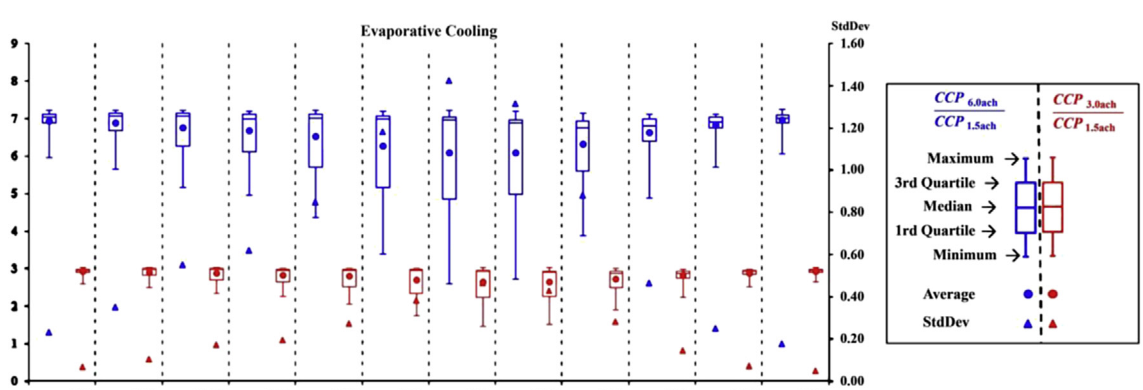

Fig. 6. Spatial statistics of CCP for evaporative cooling: ratio between CCP for 6.0 and 1.5ach (black) and between CCP for 3.0 and 1.5ach (red).(For interpretation of the references to colour in this figure legend, the reader is referred to the web version of this article.)

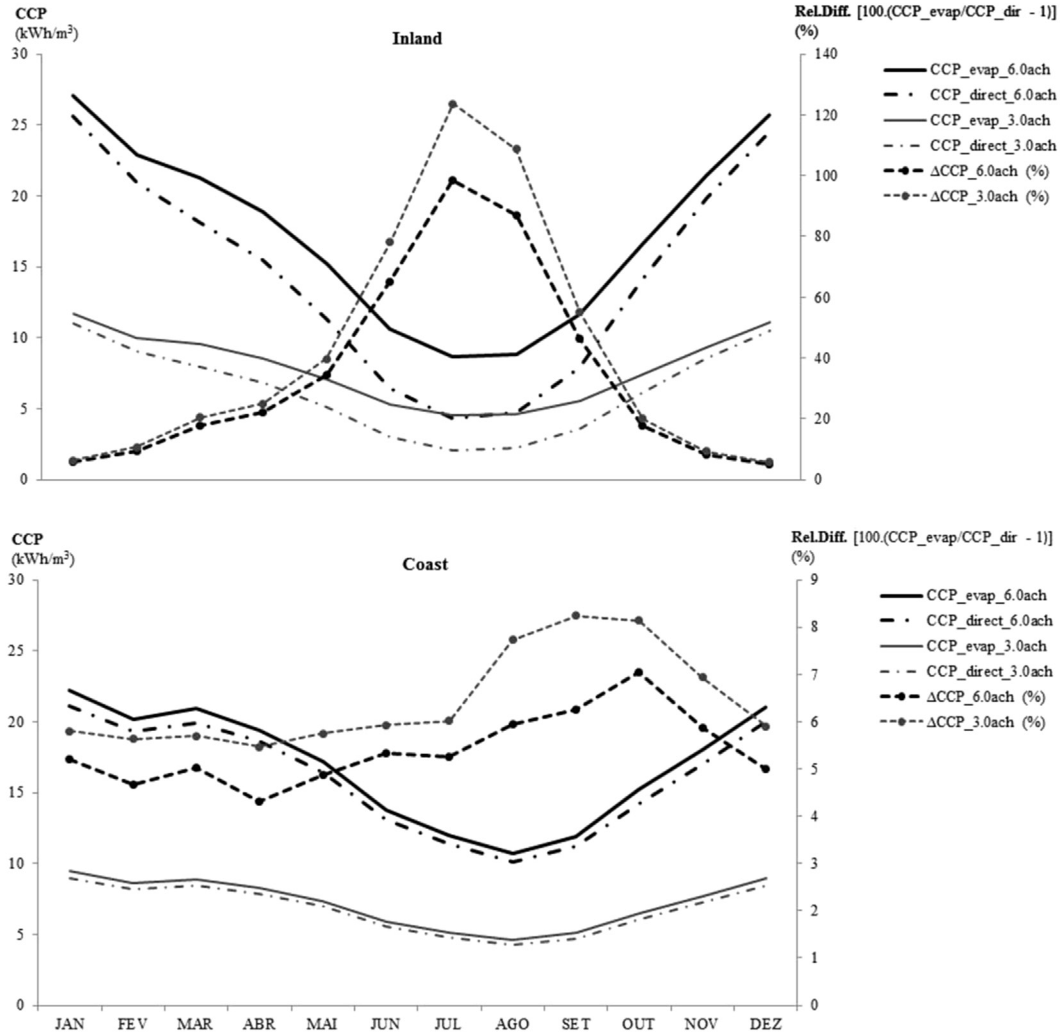

Fig. 7. CCP (left axis) and CCP's relative difference between evaporative cooling and direct ventilation (right axis) in an inland (top) and a coastal region (bottom) for different rates of ventilation.

(activated when direct radiation on the façade exceeds 10 W/m^2: overall g-value of 13%). The simulation was conducted for the month of August yielding a cooling demand of 183 kWh (3.7 kWh/m^3, 9.1 kWh/m^2) for building "A" and 66 kWh (1.3 kWh/m^3, 3.3 kWh/m^2) for building "B".

Checking the top panel of Figs. 1 and 2 (for direct ventilation and evaporative cooling, respectively) in the region of Lisbon, it can be seen that CCP is between 1 kWh/m^3 and 1.5 kWh/m^3 for direct ventilation and between 1.5 kWh/m^3 and 2 kWh/m^3 for evaporative cooling.

Thus, for building "A", direct ventilation can offer a cooling demand saving between 27% and 40%, and evaporative cooling between 40% and 54%. For the case of building "B", direct ventilation can offer a cooling demand saving between 76% and 100%, and the expected savings for the evaporative cooling system is of 100%. Nevertheless, it is important to note that the exclusive use of solar protection can bring the cooling demand down by 64% which is more than direct ventilation or evaporative cooling can offer for the selected air flow.

To assess the CCP for different rates of ventilation one can use the method above along with Figs. 5 and 6. For building "A", inspecting Fig. 5, it can be seen that for 3.0ach direct ventilation's air flow rate, the CCP value in the month of August is 2.2–3.5 times higher than the CCP value for 1.5ach, which results in 59%–100% cooling demand savings. For the case of an air flow rate of 6.0ach, the expected UCP is at least 4.7 times higher than the UCP for 1.5ach, resulting in 100% cooling demand savings. For the case of evaporative cooling, the 3.0ach air flow results in a CCP's increase from 1.6 to 3.1 times, this implies an increase from 64% to 100% in cooling demand savings. For the case of a 6.0ach air flow, the expected increase in cooling demand savings is of 100%.

5. Conclusions

In the present paper we propose a new methodology to compute the cooling demand savings for any ventilated passive cooling system for any building and spatiotemporal scale. Here, this methodology is performed for two passive cooling systems, direct ventilation and evaporative cooling, for different air flow rates and using a high quality climate dataset regarding the Iberian Peninsula. The latter was produced using a state-of-the art regional climate model, at 9 km resolution for a 19 years period, with hourly data output. We apply this procedure to the Iberian Peninsula, and thoroughly explore the benefits and caveats of both systems, comparing their potentials and their sensitivity to air flow rates. The approach is based on the calculation of the climate cooling potential and its relation with the building cooling demand.

The monthly values of the climatic cooling potential are temporally and spatially heterogeneous both for direct ventilation and evaporative cooling. Evaporative cooling always provides greater potential for the same time periods no matter the location in the Iberian Peninsula.

There is a clear asymmetry between the northern and southern part of the Iberian Peninsula regarding the potential for both direct ventilation and evaporative cooling, with higher potential values in the northern part.

Evaporative cooling provides a less heterogeneous annual cycle of climatic cooling potential, except for the areas confined to the coast and the semi-arid regions. Generally, evaporative cooling provides greater potential values than direct ventilation, but this property lessens during the winter and increases during summer, when the potential is of greater interest. Nevertheless, in some coastal regions, evaporative cooling provides less than 10% rise on the climatic cooling potential compared to direct ventilation.

The relation between the CCP provided by the different systems is of great importance for trying to understand the best system to implement in a given region, both from efficiency and economic stand points. Evaporative cooling systems have higher investment and maintenance costs. Obviously, the gain associated to evaporative compared to direct ventilation has to compensate the investment and maintenance costs. For both systems a nonlinear behaviour is found between the climatic cooling potential and the air flow rate.

Finally, the innovating methodology presented can be applied for any observational dataset or RCMs results, permitting the assessment of the climate change impact on the different passive cooling systems, and on the strategic decisions concerning their implementation, and therefore boosting the use of the renewable energy resources as a direct source of clean energy to be used in the greatest energy consuming sector, the sector of buildings: one can easily use the present study for an estimation of cooling demand savings provided by an evaporative cooling and/or a direct ventilation system in any building located in the IP, which in turn, will serve as an incentive for the implementation of such a systems in a simplified way, without the need for a complex analysis or to master thermal simulation tools, which require expertise, are a time consuming process, and require solid knowledge on the passive systems, slowing down the process of implementation and increase its costs.

Acknowledgements

Hugo Campaniço gratefully acknowledges the Ministry of Science, Technology and Higher Education of Portugal for financing this project through the Doctoral grant SFRH/BD/51329/2010. Cardoso, RM was supported by EUPORIAS - 7th Framework Programme for Research, Grant Agreement 308291.

References

[1] Energy, Transport and Environmental Indicators, Eurostat Pocketbooks, 2013 edition, ISSN 1725–4566.
[2] Jérôme Adnot, et al., EERAC – Energy Efficiency in Room Air Conditioners Ecole des Mines de Paris – Armines, France, 1999.
[3] P. Rivière, et al, Sustainable Industrial Policy – Building on the Ecodesign Directive. Final report of task 2, Air-conditioning Prod., July 2012. Study for the European Commission Directorate-General for Enterprise & Industry (DG Enterprise), contract ENTR/B1/35-2009/LOT6/SI2.549494.
[4] B. Aebischer, M. Jakob, G. Henderson, M. Jakob, G. Catenazzi, Impact of climate change on thermal comfort, heating and cooling energy demand in Europe, in: Proceedings Eceee 2007 Summer Study "Saving Energy – Just do it!", 4–9 June 2007. La Colle sur Loup, France. ISBN: 978-91-633-0899-4.
[5] B. Aebischer, G. Henderson, G. Catenazzi, Impact of climate change on energy demand in the Swiss service sector – and application to Europe, in: P. Bertoldi, B. Atanasiu (Eds.), "Improving Energy Efficiency in Commercial Buildings". Proceeding of the International Conference IEECB'06, Frankfurt, Germany, 26/27 April 2006. European Communities, EUR 22316 EN, ISBN 92-79-02748-4.
[6] Mattheos Santamouris, Dionysia Kolokotsa, Passive cooling dissipation techniques for buildings and other structures: the state of the art, Energy Build. 57 (2013) 74–94.
[7] D.G. Leo Samuel, S.M. Shiva Nagendra, M.P. Maiya, Passive alternatives to mechanical air conditioning of building: a review, Build. Environ. 66 (2013) 54–64.
[8] Ben Richard Hughes, Hassam Nasarullah Chaudhry, Saud Abdul Ghani, A review of sustainable cooling technologies in buildings, Renew. Sustain. Energy Rev. 15 (2011) 3112–3120.
[9] N. Artmann, H. Manz, P. Heiselberg, Climatic potential for passive cooling of buildings by night-time ventilation in Europe, Appl. Energy 84 (2007) 187–201.
[10] P. Hollmuller, P. Gallinelli, B. Lachal, W. Weber, Extensive sensitivity analysis of diverse ventilation cooling techniques for a typical administrative building in Mid-European climate, in: Eurosun 2008, 1st International Conference on Solar Heating, Cooling and Buildings, 7–10 October 2008, Lisbon, Portugal, 2008.
[11] V. Geros, M. Santamouris, A. Tsangrasoulis, G. Guarracino, Experimental evaluation of night ventilation phenomena, Energy Build. 29 (1999) 141–154.
[12] V. Geros, M. Santamouris, S. Karatasou, A. Tsangrassoulis, N. Papanikolaou, On the cooling potential of night ventilation techniques in the urban environment, Energy Build. 37 (2005) 243–257.
[13] M. Santamouris, A. Sfakianaki, K. Pavlou, On the efficiency of night ventilation techniques applied to residential buildings, Energy Build. 42 (2010) 1309–1313.
[14] M. Santamouris, A. Argiriou, E. Dascalaki, C. Balaras, A. Gaglia, Energy characteristics and savings potential in office buildings, Sol. Energy 52 (1) (January 1994) 59–66.
[15] Hoy-Yen Chan, Saffa B. Riffat, Jie Zhu, Review of passive solar heating and cooling technologies, Renew. Sustain. Energy Rev. 14 (2) (February 2010) 781–789.
[16] Ghassem Heidarinejad, Mojtaba Bozorgmehr, Shahram Delfani, Jafar Esmaeelian, Experimental investigation of two-stage indirect/direct evaporative cooling system in various climatic conditions, Build. Environ. 44 (2009) 2073–2079.
[17] Shahram Delfania, Jafar Esmaeeliana, Hadi Pasdarshahrib, Maryam Karamia, Energy saving potential of an indirect evaporative cooler as a pre-cooling unit for mechanical cooling systems in Iran, Energy Build. 42 (2010) 2169–2176.
[18] Moien Farmahini-Farahani, Shahram Delfani, Jafar Esmaeelian, Exergy analysis of evaporative cooling to select the optimum system in diverse climates, Energy 40 (2012) 250–257.
[19] Min-Hwi Kim, Jae-Weon Jeong, Cooling performance of a 100% outdoor air system integrated with indirect and direct evaporative coolers, Energy 52 (2013) 245–257.
[20] Zhiyin Duan, Changhong Zhan, Xingxing Zhang, Mahmud Mustafa, Xudong Zhao, Behrang Alimohammadisagvand, Ala Hasan, Indirect evaporativecooling: past, present and future potentials, Renew. Sustain. Energy Rev. 16 (2012) 6823–6850.
[21] R. Belarbi, F. Allard, Development of feasibility approaches for studying the behavior of passive cooling systems in buildings, Renew. Energy 22 (2001) 507–524.
[22] V.I. Hanby, S.Th Smith, Simulation of the future performance of low-energy evaporative cooling systems using UKCP09 climate projections, Build. Environ. 55 (2012) 110–116.
[23] A.-T. Nguyen, S. Reiter, A climate analysis tool for passive heating and cooling strategies in hot humid climate based on typical meteorological year data sets, Energy Build. (2012), http://dx.doi.org/10.1016/j.enbuild.2012.08.050.
[24] Hugo Campaniço, Pierre Hollmuller, Pedro M.M. Soares, Assessing energy savings in cooling demand of buildings using passive cooling systems based on ventilation, Appl. Energy 134 (2014) 426–438.
[25] S.M. Uppala, et al., The ERA-40 re-analysis, Q. J. R. Meteorol. Soc. 131 (2005) 2961–3012.
[26] P. Berrisford, D. Dee, K. Fielding, M. Fuentes, P. Kallberg, S. Kobayashi, S. Uppala, The ERA-interim Archive. ERA Report Series. 1, Technical Report, European Centre for Medium-Range Weather Forecasts, Shinfield Park, Reading, 2009.
[27] E. Kalnay, et al., The NCEP/NCAR 40-year reanalysis project, Bull. Am. Meteor. Soc. 77 (1996) 437–471.
[28] G.P. Compo, J.S. Whitaker, P.D. Sardeshmukh, N. Matsui, B.J. Allan, X. Yin, B.E. Gleason, R.S. Vose, G. Rutledge, et al., The twentieth century reanalysis project, Q. J. R. Meteorol. Soc. 137 (2011) 1–28, http://dx.doi.org/10.1002/qj.776.
[29] G.A. Meehl, T.F. Stocker, W.D. Collins, P. Friedlingstein, et al., Global climate projections, in: S. Solomon, D. Qin, M. Manning, Z. Chen, M. Marquis, K.B. Averyt, M. Tignor, H.L. Miller (Eds.), Climate Change 2007: The Physical Science Basis. Contribution of Working Group I to the 4th Assessment Report of the IPCC, Cambridge University Press, Cambridge, 2007, pp. 747–846.
[30] H.J. Fowler, S. Blenkinshop, C. Tebaldi, Linking climate change modelling to impacts studies: recent advances in downscaling techniques for hydrological modeling, Int. J. Climatol. 27 (2007) 1547–1578.
[31] R.E. Dickinson, R.M. Errico, F. Giorgi, G.T. Bates, A regional climate model for western United States, Clim. Change 15 (1989) 383–422.

[32] F. Giorgi, G.T. Bates, The climatological skill of a regional model over complex terrain, Mon. Weather Rev. 117 (1989) 2325–2347.
[33] J.L. McGregor, Regional climate modelling, Meteorol. Atmos. Phys. 63 (1997) 105–117.
[34] J.H. Christensen, O.B. Christensen, A summary of the PRUDENCE model projections of changes in European climate during this century, Clim. Change 81 (2007) 7–30.
[35] P.M.M. Soares, R.M. Cardoso, P.M.A. Miranda, P. Viterbo, M. Belo-Pereira, Assessment of the ENSEMBLES regional climate models in the representation of precipitation variability and extremes over Portugal, J. Geophys. Res. 117 (2012), http://dx.doi.org/10.1029/2011JD016768. D07114.
[36] F. Giorgi, L.O. Mearns, Approaches to regional climate change simulation: a review, Rev. Geophys. 29 (1991) 191–216.
[37] F. Giorgi, L. Mearns, Introduction to special section: regional climate modeling revisited, J. Geophys. Res. 104 (D6) (1999) 6335–6352.
[38] R. Laprise, Regional climate modeling, J. Comput. Phys. 227 (2008) 3641–3666, http://dx.doi.org/10.1016/j.jcp.2006.10.024.
[39] Y. Wang, L.R. Leung, J.L. McGregor, D.-K. Lee, W.-C. Wang, et al., Regional climate modelling: progress, challenges, and prospects, J. Meteorol. Soc. Jpn. 82 (2004) 1599–1628.
[40] P.M.M. Soares, R.M. Cardoso, A. Semedo, M.J. Chinita, R. Ranjha, Climatology of Iberia Coastal Low-Level Wind Jet: WRF high resolution results, Tellus A 66 (2014) 22377, http://dx.doi.org/10.3402/tellusa.v66.22377.
[41] J.H. Christensen, T.R. Carter, F. Giorgi, PRUDENCE employs new methods to assess European climate change, EOS 83 (2002) 147.
[42] P. Van der Linden, J.F.B. Mitchell (Eds.), E ENSEMBLES: Climate Change and its Impacts: Summary of Research and Results from the ENSEMBLES Project, Met Office Hadley Centre, FitzRoy Road, Exeter EX1 3 PB, UK, 2009, 160 pp.
[43] W.C. Skamarock, et al., A Description of the Advanced Research WRF Version 3, 2008. NCAR tech. note TN-475_STR, 113 pp.
[44] M.S. Bukovsky, D.J. Karoly, Precipitation Simulations Using WRF as a nested regional climate model, J. Appl. Meteor. Climatol. 48 (2009) 2152–2159, http://dx.doi.org/10.1175/2009JAMC2186.1.
[45] P.M. Caldwell, H.-N.S. Chin, D.C. Bader, G. Bala, Evaluation of a WRF based dynamical downscaling simulation over California, Clim. Change 95 (2009) 499–521.
[46] E. Flaounas, S. Bastin, S. Janicot, Regional climate modelling of the 2006 West African monsoon: sensitivity to convection and planetary boundary layer parameterisation using WRF, Clim. Dyn. 36 (2011) 1083–1105, http://dx.doi.org/10.1007/s00382-010-0785-3.
[47] L.R. Leung, Y. Qian, Atmospheric rivers induced heavy precipitation and flooding in the western U.S. simulated by the WRF regional climate model, Geophys. Res. Lett. 36 (2009) L03820, http://dx.doi.org/10.1029/2008GL036445.
[48] X.Z. Liang, H.I. Choi, K.E. Kunkel, Y. Dai, E. Joseph, J.X.L. Wang, Surface boundary conditions for mesoscale regional climate models, Earth Interact. 9 (2005).
[49] J.C.F. Lo, Z.L. Yang, R.A. Pielke Sr., Assessment of three dynamical climate downscaling methods using the Weather Research and Forecasting (WRF) model, J. Geophys. Res. 113 (2008) D09112, http://dx.doi.org/10.1029/2007JD009216.
[50] Y. Zhang, V. Dulière, P. Mote, E.P. Salathé Jr., Evaluation of WRF and HadRM mesoscale climate simulations over the United States Pacific Northwest, J. Clim. 22 (2009) 5511–5526.
[51] U. Heikkilä, A. Sandvik, A. Sorterberg, Dynamical downscaling or ERA-40 in complex terrain using WRF regional climate model, Clim. Dyn. (2010), http://dx.doi.org/10.1007/s00382-010-0928-6.
[52] A. Rios-Entenza, P.M.M. Soares, R.M. Trigo, R.M. Cardoso, G. Miguez-Macho, Moisture recycling in the Iberian Peninsula from a regional climate simulation: Spatiotemporal analysis and impact on the precipitation regime, J. Geophys. Res. Atmos. 119 (10) (2014) 5895–5912, http://dx.doi.org/10.1002/2013JD021274.
[53] P.M.M. Soares, R.M. Cardoso, P.M.A. Miranda, J. de Medeiros, M. Belo-Pereira, F. Espirito-Santo, WRF high resolution dynamical downscaling of ERA-Interim for Portugal, Clim. Dyn. 39 (2012) 2497–2522, http://dx.doi.org/10.1007/s00382-012-1315-2.
[54] R.M. Cardoso, P.M.M. Soares, P.M.A. Miranda, M. Belo-Pereira, WRF high resolution simulation of Iberian mean and extreme precipitation climate, Int. J. Climatol. 33 (11) (2013) 2591–2608, http://dx.doi.org/10.1002/joc.3616.
[55] William A. Beckman, Lars Broman, Alex Fiksel, Sanford A. Klein, Eva Lindberg, Mattias Schuler, Jeff Thornton, TRNSYS The most complete solar energy system modeling and simulation software, Renew. Energy 5 (1–4) (August 1994) 486–488.